**Proceedings of the ASME 2011 International Design Engineering Technical Conferences &
Computers and Information in Engineering Conference
IDETC/CIE 2011
August 28-31, 2011, Washington, DC, USA**

DETC2011-48147

A COORDINATE-FREE APPROACH TO TRACING THE COUPLER CURVES OF PIN-JOINTED LINKAGES

Nicolás Rojas* **and Federico Thomas**
Institut de Robòtica i Informàtica Industrial (CSIC-UPC)
Llorens Artigas 4-6, 08028 Barcelona, Spain
{nrojas, fthomas}@iri.upc.edu

ABSTRACT

In general, high-order coupler curves of plane mechanisms cannot be properly traced by standard predictor-corrector algorithms due to drifting problems and the presence of singularities. Instead of focusing on finding better algorithms for tracing curves, a simple coordinate-free method that first traces these curves in a distance space and then maps them onto the mechanism workspace is proposed. Tracing a coupler curve in the proposed distance space is much simpler because (a) the equation of this curve in this space can be straightforwardly obtained from a sequence of bilaterations; and (b) the curve in this space naturally decomposes into branches in which the signs of the oriented areas of the triangles involved in the aforementioned bilaterations remain constant. A surjective mapping permits to map the thus traced curves onto the workspace of the mechanism. The advantages of this two-step method are exemplified by tracing the coupler curves of a double butterfly linkage, curves that can reach order 48.

1 INTRODUCTION

The mechanisms considered under the title *linkwork, linkages,* or *articulated systems* are plane mechanisms involving turning pairs only. That is, sets of plane links articulated through pins. For mechanisms of this type, the equation of the curve generated by an arbitrary point on the mechanism —called the tracer point— can be obtained by solving a finite number of simultaneous equations expressing constancy of distance between pin centers which include the tracer point. Then, the coordinates of all moving pin points, other than those of the tracer, can be seen as unknowns. If we only considered single-degree-of-freedom mechanisms, the number of independent quadratic equations will exceed the number of unknowns by unity. The curve generated by the tracer point is, therefore, the eliminant of these equations. This reasoning permits to conclude that the curve generated by any point on a plane pin-jointed mechanism, possessing a finite number of links of finite size, is necessarily algebraic [1]. The same result can be attained, in a more compact way, by computing the eliminant of the set of independent loop equations after tangent-half-angle substitutions [2]. Herein we propose a radical different approach that relies on a coordinate-free formulation. Under this approach the curve generated by a tracer, the *coupler curve*, is first generated in a space of squared distances, and hence independent from the chosen reference frame, and then mapped onto the workspace of the mechanism. It will be shown how this two-step approach has two main advantages:

1. The equation of the coupler curve in the space of distances can be straightforwardly obtained from a sequence of bilaterations; and
2. The coupler curve is naturally decomposed into branches in which the signs of the oriented areas of the triangles involved in the aforementioned bilaterations remain constant.

Both advantages lead to a powerful technique for tracing coupler curves because of its simplicity while retaining the geometric flavor of the problem contrarily to what happens to the fully algebraic current approaches.

*Address all correspondence to this author.

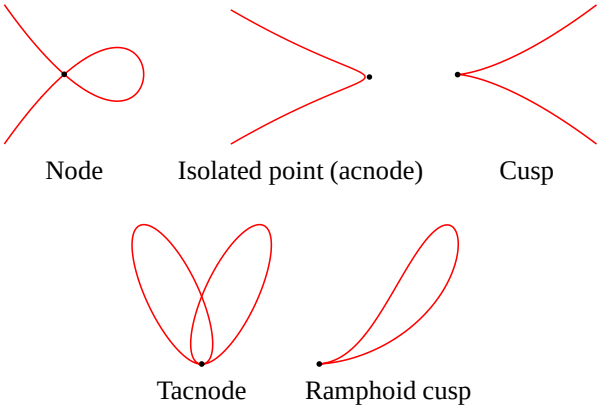

FIGURE 1. Some types of singular points of algebraic plane curves: node, isolated point, cusp, tacnode, and ramphoid cusp.

An algebraic plane curve is defined as the *root locus*, of the nonlinear equation $f(x_1,x_2)=0$ with $f:\mathbb{R}^2 \implies \mathbb{R}$ a bivariate polynomial [3]. Such root locus is a group of manifold curves joined through singular points —*i.e.*, points where the x_1 and x_2 partial derivatives of f are both zero. Figure 1 shows some types of singular points of algebraic plane curves [4].

The problem of tracing plane curves is essentially that of connecting sampled points to give rise to the graph of a curve. However a wider definition includes the computation of singular points. *Continuation methods* are one of the major approaches reported in the literature to determine the shape of a curve [5]. Since, in our case, the curves to be traced are algebraic, *polynomial continuation* can be used [6]. Other important approaches include the ones based on interval methods [7, 8]. The main advantage of these methods is that they are *global*. That is, they are able to plot the whole root locus of $f(x,y)=0$ but, depending on the application, one does not need to trace the whole root locus, but rather one of its connected components starting from a given point. Actually, this is the encountered problem when simulating the motion of a plane mechanism [9]. In this case, a very popular method is the so-called *predictor-corrector method* [3]. It consists of two major stages. In the first stage, called the predictor step, a point in the tangent line to the root locus at the current given point is estimated [Fig. 2(left)]. In the second stage, the corrector step, the predicted point is adjusted onto the curve, using typically a Newton-like method, to get a new point of the root locus [Fig. 2(right)]. In the case of closed curves, a third stage, called the filling step, is implemented to avoid overlaps.

The predictor-corrector algorithm is simple to implement and hence its popularity [9]. Unfortunately, it exhibits, in general, the undesirable phenomenon known as *drifting* in which the procedure fails to keep moving along a given branch of the curve and drift to another [Fig. 3(left)]. In most dramatic cases this might even lead to cycling [Fig. 3(right)]. This drawback can be resolved using more sophisticated mathematical tools, than the

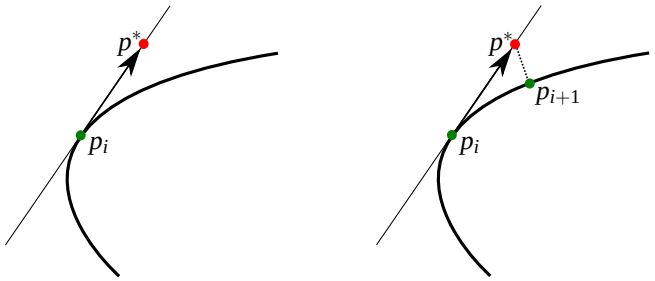

FIGURE 2. Left: In the predictor step, a point p^* in the tangent line at the current point p_i to the root locus is estimated. Right: In the corrector step, the predicted point p^* is adjusted onto the curve producing a new point p_{i+1}.

first order approximations used in standard predictor-corrector algorithms, such as Runge-Kutta or Adam's method [10].

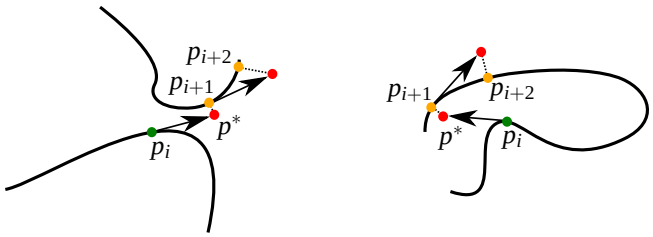

FIGURE 3. Left: The drifting problem. Right: The cycling problem. Adapted from [3].

Another important drawback of predictor-corrector algorithms arises when the plane curve to be traced has singular points because the tangent is undefined. An approach to overcome this issue is by first computing the singular points with symbolic processing techniques for then use them as starting points of a predictor-corrector algorithm. A simpler and more elegant alternative is the use of derivative-free methods such as the Morgado-Gomes false position numerical method [11].

The possibility of drifting, cycling, and having problems with singular points, increases dramatically with the order of the curve to be traced because the number of branches into which the curve is divided, the number of singular points, and the number of loops, grow accordingly. This is the case of the coupler curves of pin-jointed linkages. For example, the coupler curve of the well-known four-bar linkage is a sextic [12] and that of the double butterfly linkage is of forty-eight order [13]. In this paper, instead of focusing on a better algorithm for tracing coupler curves able to deal with all mentioned problems in the workspace of the mechanism, a simple coordinate-free method that first traces the coupler curve in a distance space and then maps it onto the workspace is proposed. Since this mapping is surjective and trac-

ing a curve in the proposed distance space is much simpler than tracing the corresponding coupler curve in the workspace of the mechanism, the proposed two-step strategy proves to provide an important simplification.

This paper is structured as follows. Section II briefly reviews how to obtain distance ratios in trees of triangles through bilaterations, the basic operation required to derive our coordinate-free formulation. Section III concentrates on the case study of tracing the coupler curves of a double butterfly linkage. A numerical example is next presented that leads to complex coupler curves which would be very difficult to be traced by a standard predictor-corrector algorithm. The main results are summarized in Section IV.

2 THE COORDINATE-FREE APPROACH

2.1 Bilateration

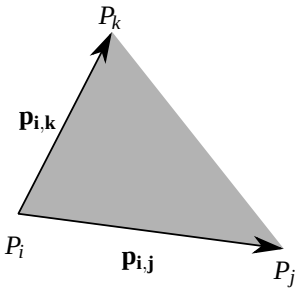

FIGURE 4. The bilateration problem in $\mathbb{R}^2$.

The bilateration problem consists of finding the feasible locations of a point, say P_k, given its distances to two other points, say P_i and P_j, whose locations are known. Then, according to Fig. 4, the result, in matrix form, can be expressed as:

$$\mathbf{p}_{i,k} = \mathbf{Z}_{i,j,k}\,\mathbf{p}_{i,j} \tag{1}$$

where

$$\mathbf{Z}_{i,j,k} = \frac{1}{D(i,j)}\begin{bmatrix} D(i,j;i,k) & \mp\sqrt{D(i,j,k)} \\ \pm\sqrt{D(i,j,k)} & D(i,j;i,k) \end{bmatrix}, \tag{2}$$

is called a *bilateration matrix*, and

$$D(i_1,\ldots,i_n;j_1,\ldots,j_n) = 2\left(\frac{-1}{2}\right)^n \begin{vmatrix} 0 & 1 & \ldots & 1 \\ 1 & s_{i_1,j_1} & \ldots & s_{i_1,j_n} \\ \vdots & \vdots & \ddots & \vdots \\ 1 & s_{i_n,j_1} & \ldots & s_{i_n,j_n} \end{vmatrix} \tag{3}$$

with $s_{i,j} = d_{i,j}^2 = \left\|\mathbf{p}_{i,j}\right\|^2$, where $\mathbf{p}_{i,j} = \mathbf{p}_j - \mathbf{p}_i = \overrightarrow{P_iP_j}$. This determinant is known as the *Cayley-Menger bi-determinant* of the point sequences $P_{i_1},\ldots,P_{i_n}$, and $P_{j_1},\ldots,P_{j_n}$ and its geometric interpretation plays a fundamental role in the so-called Distance Geometry [14]. When the two point sequences are the same, it is convenient to abbreviate $D(i_1,\ldots,i_n;i_1,\ldots,i_n)$ by $D(i_1,\ldots,i_n)$, which is simply called the *Cayley-Menger determinant* of the involved points. The interested reader is addressed to [15] for a detailed derivation of the above formulas.

Now, it is important to observe that bilateration matrices constitute an Abelian group under product and addition —*i.e.*, these kind of matrices commute under these operations— and if $\mathbf{v} = \mathbf{Z}\mathbf{w}$, where $\mathbf{Z}$ is a bilateration matrix, then $\|\mathbf{v}\|^2 = \det(\mathbf{Z})\,\|\mathbf{w}\|^2$.

2.2 Distance ratios in trees of triangles

A tree of triangles is defined as a set of triangles that are connected by their edges such that any two triangles are connected by a single strip of triangles —*i.e.*, a series of connected triangles that share one edge with one neighbor and another with the next (Fig. 5). Note that this definition includes cases in which edges are shared by more than two triangles.

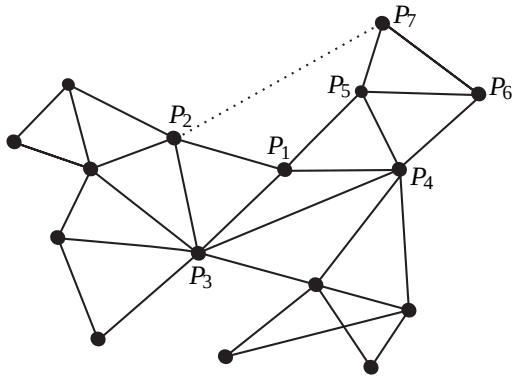

FIGURE 5. In a tree of triangles, the distance ratio between two couples of vertices can be obtained by a set of bilaterations (see text for details).

In a tree of triangles, it is straightforward to find the ratio between any two distances involving any couple of vertices using sequences of bilaterations. This is better explained through an example. Let us suppose that we are interested in finding $\frac{s_{5,7}}{s_{1,2}}$ in the tree of triangles of Fig. 5. The corresponding edges are connected by the strip of triangles $\{P_1P_2P_3, P_1P_3P_4, P_1P_4P_5, P_5P_4P_6, P_5P_6P_7\}$. Then, taking the segment P_1P_2 as reference, we can perform the following sequence

of bilaterations:

$$\mathbf{p}_{1,4} = \mathbf{Z}_{1,3,4}\,\mathbf{Z}_{1,2,3}\,\mathbf{p}_{1,2} \tag{4}$$

$$\begin{aligned}\mathbf{p}_{1,5} &= \mathbf{Z}_{1,4,5}\,\mathbf{p}_{1,4} \\ &= \mathbf{Z}_{1,4,5}\,\mathbf{Z}_{1,3,4}\,\mathbf{Z}_{1,2,3}\,\mathbf{p}_{1,2}\end{aligned} \tag{5}$$

$$\begin{aligned}\mathbf{p}_{1,6} &= (\mathbf{I} - \mathbf{Z}_{4,5,6}\,\mathbf{Z}_{4,1,5})\,\mathbf{p}_{1,4} \\ &= (\mathbf{I} - \mathbf{Z}_{4,5,6}\,\mathbf{Z}_{4,1,5})\,\mathbf{Z}_{1,3,4}\,\mathbf{Z}_{1,2,3}\,\mathbf{p}_{1,2}.\end{aligned} \tag{6}$$

Thus,

$$\begin{aligned}\mathbf{p}_{5,7} &= \mathbf{Z}_{5,6,7}\,\mathbf{p}_{5,6} = \mathbf{Z}_{5,6,7}\,(-\mathbf{p}_{1,5} + \mathbf{p}_{1,6}) \\ &= \mathbf{Z}_{5,6,7}\big(-\mathbf{Z}_{1,4,5} + \mathbf{I} - \mathbf{Z}_{4,5,6}\,\mathbf{Z}_{4,1,5}\big)\mathbf{Z}_{1,3,4}\,\mathbf{Z}_{1,2,3}\,\mathbf{p}_{1,2}.\end{aligned} \tag{7}$$

As a consequence,

$$\frac{s_{5,7}}{s_{1,2}} = \det\Big(\mathbf{Z}_{5,6,7}\big(-\mathbf{Z}_{1,4,5} + \mathbf{I} - \mathbf{Z}_{4,5,6}\,\mathbf{Z}_{4,1,5}\big)\mathbf{Z}_{1,3,4}\,\mathbf{Z}_{1,2,3}\Big).$$

Now, let us suppose that we want to compute $\frac{s_{2,7}}{s_{1,2}}$. In this case P_2P_7 is not an edge of any triangle in the tree but clearly

$$\mathbf{p}_{2,7} = -\mathbf{p}_{1,2} + \mathbf{p}_{1,5} + \mathbf{p}_{5,7}.$$

Then, the substitution of (5) and (7) in the above equation yields:

$$\begin{aligned}\mathbf{p}_{2,7} = &\big(-\mathbf{I} + \big(\mathbf{Z}_{1,4,5} + \mathbf{Z}_{5,6,7}\big(-\mathbf{Z}_{1,4,5} + \mathbf{I} - \mathbf{Z}_{4,5,6}\,\mathbf{Z}_{4,1,5}\big)\big) \\ &\mathbf{Z}_{1,3,4}\,\mathbf{Z}_{1,2,3}\big)\,\mathbf{p}_{1,2}.\end{aligned}$$

Therefore,

$$\begin{aligned}\frac{s_{2,7}}{s_{1,2}} = &\det\Big(-\mathbf{I} + \big(\mathbf{Z}_{1,4,5} + \mathbf{Z}_{5,6,7}\big(-\mathbf{Z}_{1,4,5} + \mathbf{I} - \mathbf{Z}_{4,5,6}\,\mathbf{Z}_{4,1,5}\big)\big) \\ &\mathbf{Z}_{1,3,4}\,\mathbf{Z}_{1,2,3}\Big).\end{aligned}$$

By proceeding in a similar way, it is possible to obtain the distance ratio between any two couples of points in the tree.

The possibility of computing distance ratios that involve arbitrary couples of vertices, using sequences of bilaterations, is not limited to trees of triangles. This can also be applied to trees of trees, that is, trees of triangles where each tree shares two vertices with one neighboring tree and another couple with another tree. This is the case of most planar linkages [16], including the double butterfly linkage, as shown next.

3 CASE STUDY: THE DOUBLE BUTTERFLY LINKAGE

The double butterfly linkage has one of the sixteen topologies available for eight-bar single-degree-of-freedom linkages [17]. In the context of classical kinematics of mechanisms, the input-output problem for this linkage leads to either sixteenth order or eighteenth order polynomials depending on the selected fix and input links [2]. This input-output problem is equivalent to the position analysis problem of the seven-link Baranov trusses of type II and III [15]. A polynomial equation for the path of a point located in a coupler link of the double butterfly linkage was presented in [13] for the first time. The resulting polynomial was shown to be, at most, of forty-eighth order. A sampled plot of this curve is presented in [8]. The interested reader is referred to [18] for more details on this mechanism.

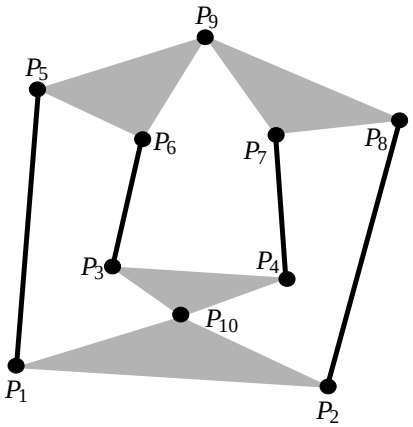

FIGURE 6. The double butterfly linkage.

Fig. 6 shows a double butterfly linkage. It consists of four binary links and four ternary links with three independent loops, any of them of the four-bar type. The centers of the revolute joints of the binary links define the line segments P_1P_5, P_3P_6, P_4P_7, and P_2P_8, and those for the ternary links define the triangles $P_1P_{10}P_2$, $P_{10}P_3P_4$, $P_6P_5P_9$, and $P_7P_9P_8$. The position analysis problem for this linkage consists in, given the dimensions of all links, calculating all possible paths traced by a point located in any coupler link, respect to a selected ground link — *i.e.*, determining the coupler curves for an inversion of the linkage.

3.1 Deriving the coordinate-free input-output equation

Instead of directly computing the relative Cartesian poses of all links through loop-closure equations, we will use distance ratios in trees of triangles to compute the set of values of $s_{2,4}$ and $s_{1,6}$ compatible with all binary and ternary links side lengths. Thus, the resulting equation is coordinate-free, algebraic (that is,

free of transcendental functions), and entirely posed in terms of distances and oriented areas.

First, according to the notation used in Fig. 6, let us calculate $s_{1,3}$ and $s_{4,9}$ as functions of $s_{2,4}$ and $s_{1,6}$. To this end, we will compute the distance ratios $\frac{s_{1,3}}{s_{2,4}}$ and $\frac{s_{4,9}}{s_{2,4}}$, respectively.

For the tree of triangles defined by $\{P_2P_{10}P_4, P_{10}P_3P_4, P_1P_{10}P_2\}$ [Fig. 7(left)], we have

$$\mathbf{p}_{2,1} = \mathbf{Z}_{2,10,1}\,\mathbf{Z}_{2,4,10}\,\mathbf{p}_{2,4} \tag{8}$$
$$\mathbf{p}_{2,3} = (\mathbf{I} - \mathbf{Z}_{4,10,3}\,\mathbf{Z}_{4,2,10})\,\mathbf{p}_{2,4}. \tag{9}$$

Therefore,

$$\mathbf{p}_{1,3} = -\mathbf{p}_{2,1} + \mathbf{p}_{2,3} = \mathbf{D}_1\,\mathbf{p}_{2,4} \tag{10}$$

where $\mathbf{D}_1 = (-\mathbf{Z}_{2,10,1}\,\mathbf{Z}_{2,4,10} + \mathbf{I} - \mathbf{Z}_{4,10,3}\,\mathbf{Z}_{4,2,10})$. As a consequence,

$$s_{1,3} = \det(\mathbf{D}_1)\,s_{2,4}. \tag{11}$$

The expansion of the above equation yields a scalar expression for $s_{1,3}$ in function of the unknown squared distance $s_{2,4}$.

For the tree of triangles defined by $\{P_1P_6P_3, P_1P_5P_6, P_5P_9P_6\}$ [Fig. 7(center)], we have

$$\mathbf{p}_{1,6} = \mathbf{Z}_{1,3,6}\,\mathbf{p}_{1,3} \tag{12}$$
$$\mathbf{p}_{1,9} = (\mathbf{I} - \mathbf{Z}_{6,5,9}\,\mathbf{Z}_{6,1,5})\,\mathbf{p}_{1,6}. \tag{13}$$

Substituting (10) into (12) and replacing the result in (13), we get

$$\mathbf{p}_{1,9} = \mathbf{D}_2\,\mathbf{p}_{2,4} \tag{14}$$

where $\mathbf{D}_2 = (\mathbf{I} - \mathbf{Z}_{6,5,9}\,\mathbf{Z}_{6,1,5})\,\mathbf{Z}_{1,3,6}\,\mathbf{D}_1$. Now, since $\mathbf{p}_{2,9} = \mathbf{p}_{2,1} + \mathbf{p}_{1,9}$ and $\mathbf{p}_{4,9} = -\mathbf{p}_{2,4} + \mathbf{p}_{2,9}$, we obtain

$$\mathbf{p}_{4,9} = (-\mathbf{I} + \mathbf{Z}_{2,10,1}\,\mathbf{Z}_{2,4,10} + \mathbf{D}_2)\,\mathbf{p}_{2,4}. \tag{15}$$

Hence,

$$s_{4,9} = \det(-\mathbf{I} + \mathbf{Z}_{2,10,1}\,\mathbf{Z}_{2,4,10} + \mathbf{D}_2)\,s_{2,4}. \tag{16}$$

The substitution of (11) into the expansion of the above equation yields a scalar expression for $s_{4,9}$ in function of $s_{1,6}$ and $s_{2,4}$.

Finally, for the tree of triangles defined by $\{P_4P_9P_7, P_7P_9P_8\}$ [Fig. 7(right)], we have

$$\mathbf{p}_{4,8} = (\mathbf{I} - \mathbf{Z}_{9,7,8}\,\mathbf{Z}_{9,4,7})\,\mathbf{p}_{4,9}. \tag{17}$$

Substituting (15) in (17), we get

$$\mathbf{p}_{4,8} = \big(\mathbf{I} - \mathbf{Z}_{9,7,8}\,\mathbf{Z}_{9,4,7}\big)\big(-\mathbf{I} + \mathbf{Z}_{2,10,1}\,\mathbf{Z}_{2,4,10} + \mathbf{D}_2\big)\mathbf{p}_{2,4}. \tag{18}$$

Then,

$$\begin{aligned}\mathbf{p}_{2,8} =& \mathbf{p}_{2,4} + \mathbf{p}_{4,8}\\ =& \big(\mathbf{I} + \big(\mathbf{I} - \mathbf{Z}_{9,7,8}\,\mathbf{Z}_{9,4,7}\big)\big(-\mathbf{I} + \mathbf{Z}_{2,10,1}\,\mathbf{Z}_{2,4,10} + \mathbf{D}_2\big)\big)\mathbf{p}_{2,4}.\end{aligned} \tag{19}$$

Therefore,

$$\frac{s_{2,8}}{s_{2,4}} = \det\Big(\mathbf{I} + \big(\mathbf{I} - \mathbf{Z}_{9,7,8}\,\mathbf{Z}_{9,4,7}\big)\big(-\mathbf{I} + \mathbf{Z}_{2,10,1}\,\mathbf{Z}_{2,4,10} + \mathbf{D}_2\big)\Big). \tag{20}$$

The expansion of the right hand side of equation (20), using (11) and (16) for substituting the unknown squared distances $s_{1,3}$ and $s_{4,9}$, respectively, yields a scalar radical equation in two variables: $s_{2,4}$ and $s_{1,6}$. The solution of this equation gives the set of values of $s_{2,4}$ and $s_{1,6}$ compatible with all binary and ternary links side lengths of the linkage.

By expanding all the Cayley-Menger determinants involved in equation (20), we get

$$\frac{s_{2,8}}{s_{2,4}} = \frac{1}{s_{2,4}\,s_{1,6}\,s_{1,3}\,s_{4,9}}\,\Psi, \tag{21}$$

that is,

$$\Psi - s_{1,6}\,s_{1,3}\,s_{4,9}\,s_{2,8} = 0,$$

where

$$\begin{aligned}\Psi =& \Psi_1 + \Psi_2 A_{2,4,10} + \Psi_3 A_{1,3,6} + \Psi_4 A_{1,6,5} + \Psi_5 A_{4,9,7}\\ &+ \Psi_6 A_{2,4,10}A_{1,3,6} + \Psi_7 A_{2,4,10}A_{1,6,5} + \Psi_8 A_{2,4,10}A_{4,9,7}\\ &+ \Psi_9 A_{1,3,6}A_{1,6,5} + \Psi_{10} A_{1,3,6}A_{4,9,7} + \Psi_{11} A_{1,6,5}A_{4,9,7}\\ &+ \Psi_{12} A_{2,4,10}A_{1,3,6}A_{1,6,5} + \Psi_{13} A_{2,4,10}A_{1,3,6}A_{4,9,7}\\ &+ \Psi_{14} A_{2,4,10}A_{1,6,5}A_{4,9,7} + \Psi_{15} A_{1,3,6}A_{1,6,5}A_{4,9,7}\\ &+ \Psi_{16} A_{2,4,10}A_{1,3,6}A_{1,6,5}A_{4,9,7},\end{aligned}$$

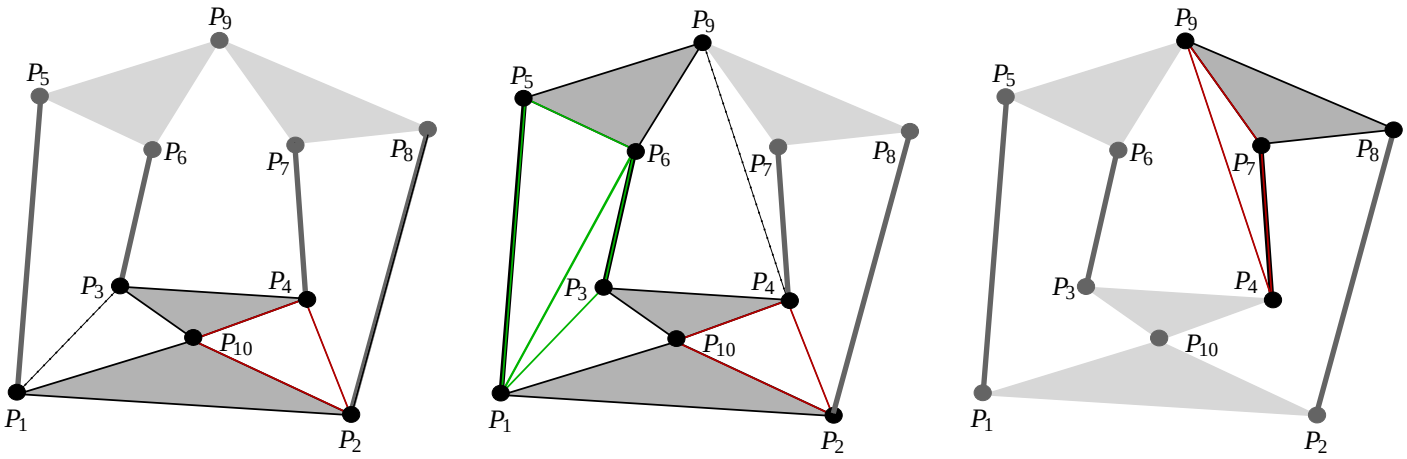

FIGURE 7. The trees of triangles involve in the computation of the coordinate-free formulation for the position analysis of a double butterfly linkage. Left: The distance ratio $\frac{s_{1,3}}{s_{2,4}}$ is computed using the tree of triangles defined by $\{P_2P_{10}P_4, P_{10}P_3P_4, P_1P_{10}P_2\}$. Center: The distance ratio $\frac{s_{4,9}}{s_{2,4}}$ is computed using the trees of triangles defined by $\{P_2P_{10}P_4, P_{10}P_3P_4, P_1P_{10}P_2\}$ and $\{P_1P_6P_3, P_1P_5P_6, P_5P_9P_6\}$. Right: The tree of triangles defined by $\{P_4P_9P_7, P_7P_9P_8\}$.

with Ψ_i, $i = 1, \ldots, 16$, polynomials in $s_{2,4}$, $s_{1,6}$, $s_{1,3}$, and $s_{4,9}$, and

$$A_{2,4,10} = \pm\frac{1}{4}\sqrt{\left[s_{2,4} - (d_{4,10} - d_{2,10})^2\right]\left[(d_{4,10} + d_{2,10})^2 - s_{2,4}\right]},$$
$$A_{1,3,6} = \pm\frac{1}{4}\sqrt{\left[s_{1,6} - (d_{3,6} - d_{1,3})^2\right]\left[(d_{3,6} + d_{1,3})^2 - s_{1,6}\right]},$$
$$A_{1,6,5} = \pm\frac{1}{4}\sqrt{\left[s_{1,6} - (d_{5,6} - d_{1,5})^2\right]\left[(d_{5,6} + d_{1,5})^2 - s_{1,6}\right]},$$
$$A_{4,9,7} = \pm\frac{1}{4}\sqrt{\left[s_{4,9} - (d_{7,9} - d_{4,7})^2\right]\left[(d_{7,9} + d_{4,7})^2 - s_{4,9}\right]},$$

the unknown oriented areas of the triangles $P_2P_4P_{10}$, $P_1P_6P_3$, $P_1P_6P_5$, $P_4P_9P_7$, respectively.

3.2 Obtaining coordinates from the coordinate-free formulation

Now, we proceed to calculate the Cartesian position of the linkage's revolute pair centers. If we are interested in the kinematic inversion of the double butterfly linkage in which the ground link is the ternary link defined by $P_1P_2P_{10}$, we have to fix the location of these three points. In this case, we can set, for instance,

$$\mathbf{p}_1 = \begin{pmatrix} 0 \\ 0 \end{pmatrix}, \mathbf{p}_2 = \begin{pmatrix} d_{1,2} \\ 0 \end{pmatrix}, \text{ and } \mathbf{p}_{10} = \begin{pmatrix} \frac{D(1,2;1,10)}{d_{1,2}} \\ \sqrt{s_{1,10} - \frac{D^2(1,2;1,10)}{s_{1,2}}} \end{pmatrix}.$$

Then, the path traced by P_3, P_4, P_5, P_6, P_7, P_8, and P_9 can be computed by replacing each previously computed ordered pair $(s_{2,4}, s_{1,6})$, as explained in the next subsection, in the set of equations:

$$\mathbf{p}_{2,4} = \mathbf{Z}_{2,10,4}\,\mathbf{p}_{2,10} \quad (22a)$$
$$\mathbf{p}_{10,3} = \mathbf{Z}_{10,4,3}\,\mathbf{p}_{10,4} \quad (22b)$$
$$\mathbf{p}_{1,6} = \mathbf{Z}_{1,3,6}\,\mathbf{p}_{1,3} \quad (22c)$$
$$\mathbf{p}_{1,5} = \mathbf{Z}_{1,6,5}\,\mathbf{p}_{1,6} \quad (22d)$$
$$\mathbf{p}_{5,9} = \mathbf{Z}_{5,6,9}\,\mathbf{p}_{5,6} \quad (22e)$$
$$\mathbf{p}_{4,7} = \mathbf{Z}_{4,9,7}\,\mathbf{p}_{4,9} \quad (22f)$$
$$\mathbf{p}_{7,8} = \mathbf{Z}_{7,9,8}\,\mathbf{p}_{7,9}. \quad (22g)$$

If we are interested in the paths traced by a coupler point different from the revolute pair centers, we could compute its Cartesian location using also a bilateration from the revolute pair centers of the corresponding coupler link.

For a different kinematic inversion, we simply have to calculate the Euclidean transformation between the fixed values of the ground link and the values computed with the set of equations (22), and use it to recompute the values for the other revolute pair centers.

The procedure described in this section obtains all possible paths traced by a coupler point of any kinematic inversion of the double butterfly linkage. It remains to identify the movement followed by the linkage when it starts from a given position, the main problem when simulating the motion of a mechanism.

3.3 Coupler curve tracing

As already mentioned, the problem of tracing a coupler curve consists in determining the path followed by a coupler

point from a given initial position. Next, a simple procedure, with a geometric flavor, is deduced from the coordinate-free equation (21). First note that this equation contains four variable oriented areas, namely, $A_{2,4,10}$, $A_{1,3,6}$, $A_{1,6,5}$, and $A_{4,9,7}$. Hence, strictly speaking, equation (21) encompasses sixteen different scalar equations, one per each combination of signs for these areas. Each set of solutions to these sixteen equations correspond to different families of assembly modes. The idea of the proposed procedure is to explode this fact for solving the coupler curve tracing problem.

Let us define

$$f_\eta(s_{2,4}, s_{1,6}) = \frac{1}{s_{2,4}\, s_{1,6}\, s_{1,3}\, s_{4,9}}\,\Psi - \frac{s_{2,8}}{s_{2,4}} \qquad (23)$$

with Ψ as defined in (21), with the unknown squared distances $s_{1,3}$ and $s_{4,9}$ substituted by the expressions in (11) and (16), respectively. $\eta = 0,\ldots,15$ specifies the combination of signs for the areas $A_{2,4,10}$, $A_{1,3,6}$, $A_{1,6,5}$, and $A_{4,9,7}$. Thus, for example, $\eta = 10 = (1010)_2$ implies that $A_{2,4,10} > 0$, $A_{1,3,6} < 0$, $A_{1,6,5} > 0$, and $A_{4,9,7} < 0$. Given an initial position for the double butterfly linkage identified by the tuple $({s_{2,4}}^{(0)}, {s_{1,6}}^{(0)}, \eta)$ where $f_\eta({s_{2,4}}^{(0)}, {s_{1,6}}^{(0)}) = 0$, the path followed by a coupler point can be traced following these steps:

1 Use a predictor-corrector method for computing a new ordered pair $({s_{2,4}}^{(k)}, {s_{1,6}}^{(k)})$ such that $f_\eta({s_{2,4}}^{(k)}, {s_{1,6}}^{(k)}) = 0$ and $|{s_{2,4}}^{(k)} - {s_{2,4}}^{(k-1)}| < \delta$, where δ is a specified resolution step.

2 Evaluate the oriented areas $A_{2,4,10}$, $A_{1,3,6}$, $A_{1,6,5}$, and $A_{4,9,7}$ with the ordered pair $({s_{2,4}}^{(k)}, {s_{1,6}}^{(k)})$. If any of them is equal to zero, the current configuration —*i.e.*, the tuple $({s_{2,4}}^{(k)}, {s_{1,6}}^{(k)}, \eta)$— belongs to more than one family of assembly modes and the linkage movement may evolve along different paths. Identify all these families, that is, determine all feasible values that η can assume.

3 Repeat steps 1 and 2 for each tuple $({s_{2,4}}^{(k)}, {s_{1,6}}^{(k)}, \eta)$ until the initial ordered pair $({s_{2,4}}^{(0)}, {s_{1,6}}^{(0)})$ is reached or it is not possible to compute any new ordered pair $({s_{2,4}}^{(k+1)}, {s_{1,6}}^{(k+1)})$.

The path traced by a coupler point of any kinematic inversion of the double butterfly linkage is computed by replacing each tuple $({s_{2,4}}^{(k)}, {s_{1,6}}^{(k)}, \eta)$ in the set of equations (22). Since the combination of signs for the areas $A_{2,4,10}$, $A_{1,3,6}$, $A_{1,6,5}$, and $A_{4,9,7}$ is determined by η, the resulting location for the revolute pair centers and the coupler point is unique.

3.4 NUMERICAL EXAMPLE

According to the notation used in Fig. 6, let us suppose that $s_{1,2} = 169$, $s_{1,5} = 145$, $s_{1,10} = 65$, $s_{2,8} = 200$, $s_{2,10} = 52$, $s_{3,4} = 5$, $s_{3,6} = 50$, $s_{3,10} = 5$, $s_{4,7} = 36$, $s_{4,10} = 10$, $s_{5,6} = 5$, $s_{5,9} = 53$, $s_{6,9} = 34$, $s_{7,8} = 10$, $s_{7,9} = 5$, and $s_{8,9} = 25$. In this case, the input variable $s_{2,4}$ lies in the interval $[62 - 4\sqrt{13}\sqrt{10}, 62 + 4\sqrt{13}\sqrt{10}]$. Figure 8(top) shows the root locus of (21) for sampled values of $s_{2,4}$ in its range using increments of $\frac{1}{100}$. The corresponding Cartesian locations for P_9, when the ground link is $P_1P_2P_{10}$ with $\mathbf{p}_1 = (4,0)^T$, $\mathbf{p}_2 = (17,0)^T$, and $\mathbf{p}_{10} = (11,4)^T$, are presented in Fig. 8(bottom). Both curves have been sampled, not traced. In

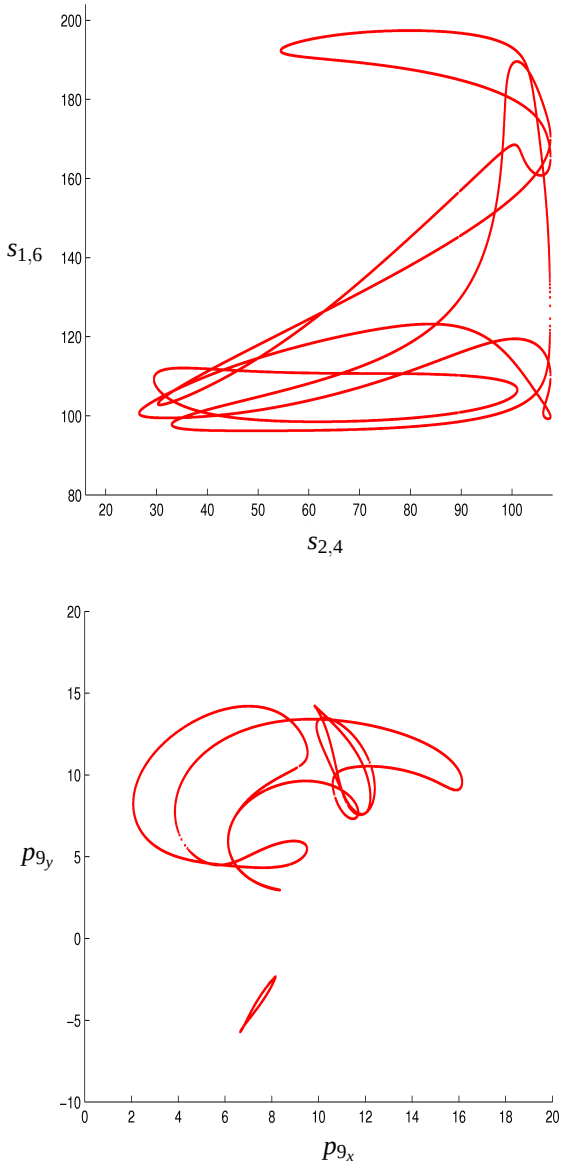

FIGURE 8. Top: The root locus of equation (21) in the plane defined by $s_{2,4}$ and $s_{1,6}$ for the analyzed double butterfly linkage. Bottom: The corresponding Cartesian locations for P_9 when the ground link is $P_1P_2P_{10}$ with $P_1 = (4,0)^T$, $P_2 = (17,0)^T$, and $P_{10} = (11,4)^T$.

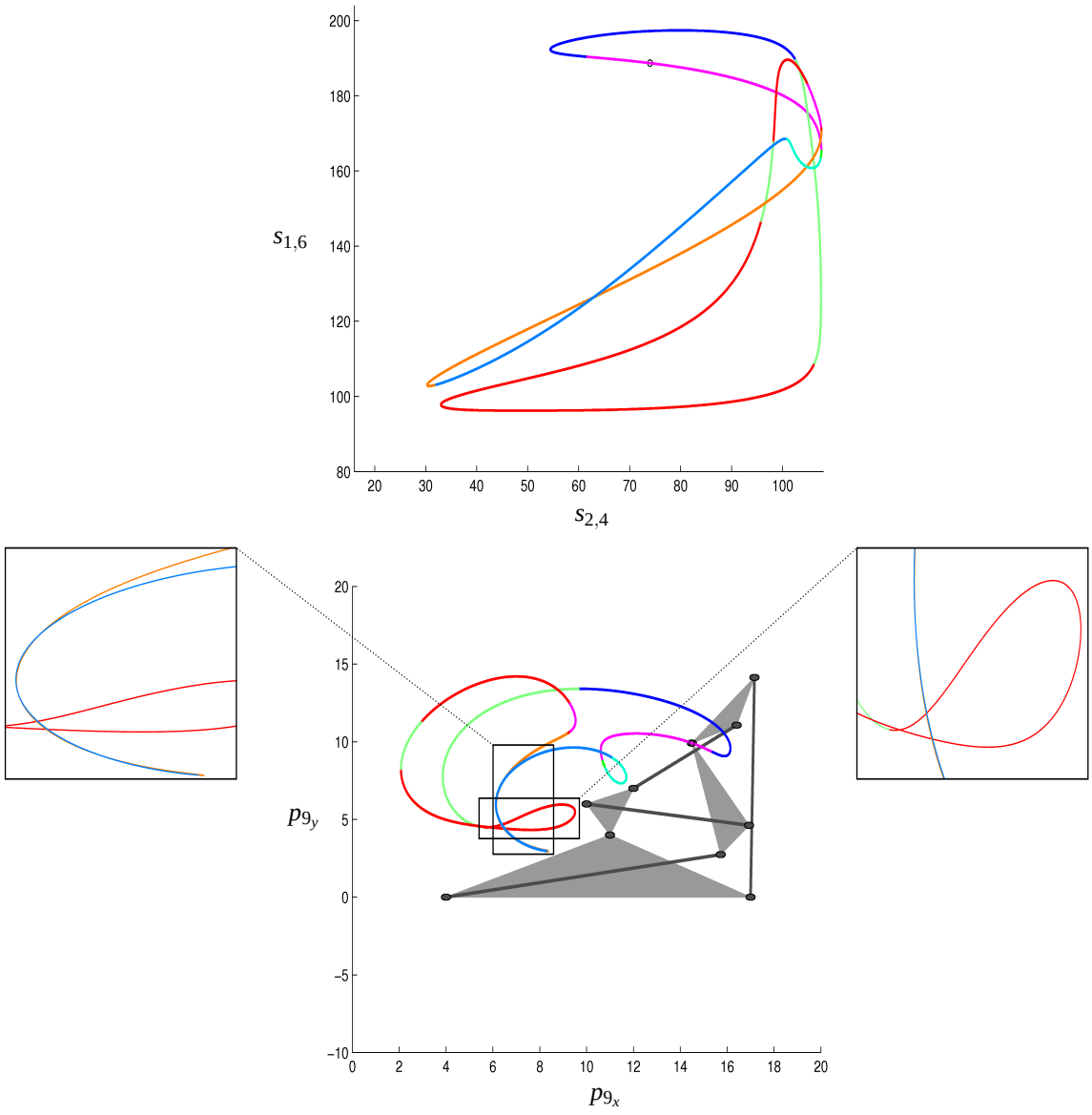

FIGURE 9. Top: Values reached by $s_{2,4}$ and $s_{1,6}$ in the analyzed double butterfly linkage when starting from the configuration $s_{2,4} = 74$, $s_{1,6} = 188.68$, and $\eta = 8$. Bottom: The corresponding Cartesian path traced by P_9. Zoomed areas show how after mapping the distance curve onto the working space a ramphoid cusp and near quadruple point are generated. The ground link is taken to be $P_1P_2P_{10}$ with $P_1 = (4,0)^T$, $P_2 = (17,0)^T$, and $P_{10} = (11,4)^T$.

other words, there is no information on the connectivity of each sample. Actually, finding this connectivity is the difficult point. These sampled curves have been computed here for comparison purposes with the results obtained by tracing as explained below.

From Fig. 8, it is clear that it is not trivial to identify the movement performed by the double butterfly linkage when it starts from a given position. Let us suppose that we are interested in the path followed by the revolute pair center P_9 from an initial configuration defined by $s_{2,4} = 74$, $s_{1,6} = 188.68$, and $\eta = 8$ (that is, $A_{2,4,10} > 0$, $A_{1,3,6} < 0$, $A_{1,6,5} < 0$, and $A_{4,9,7} < 0$). Figure 9(top) shows the distance path obtained using the procedure explained in the previous subsection and the corresponding Cartesian path is depicted in Fig. 9(bottom). In both figures, colors indicate the signs of the oriented areas according to Tab. 1.

The fact that the mapping from the distance space to the workspace is surjective (two points of the distance space can be

Color	$A_{2,4,10}$	$A_{1,3,6}$	$A_{1,6,5}$	$A_{4,9,7}$
	−	−	−	−
	−	−	−	+
	−	+	−	−
	−	+	−	+
	−	+	+	+
	+	−	−	−
	+	−	−	+
	+	+	−	−
	+	+	−	+
	+	+	+	−
	+	+	+	+

TABLE 1. Code of colors used in Figs. 9, 10, and 11 for the signs of $A_{2,4,10}$, $A_{1,3,6}$, $A_{1,6,5}$, and $A_{4,9,7}$.

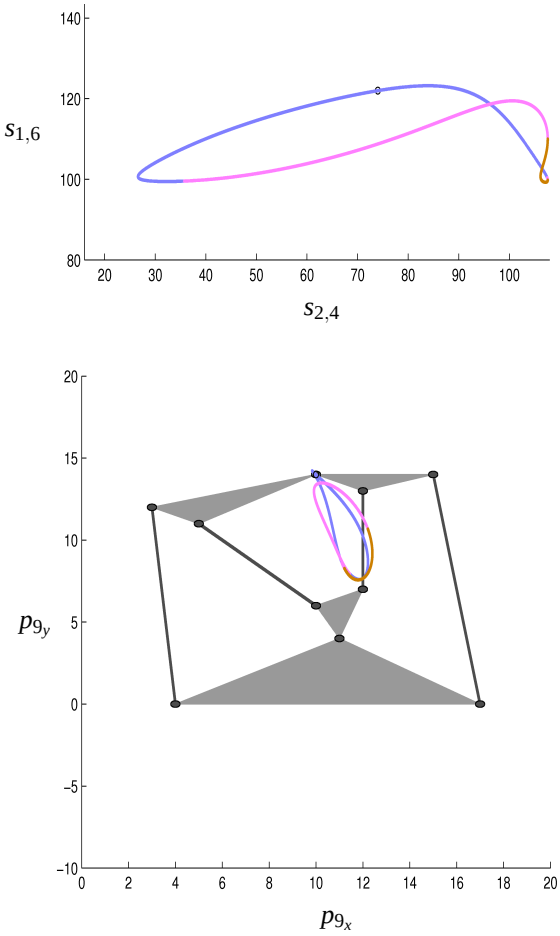

FIGURE 10. Top: Values reached by $s_{2,4}$ and $s_{1,6}$ in the analyzed double butterfly linkage when starting from the configuration $s_{2,4} = 74$, $s_{1,6} = 122$, and $\eta = 14$. Bottom: The corresponding Cartesian path traced by P_9 where a cusp and a tacnode can be identified.

mapped onto the same point in the workspace) is actually the underlying reason that makes coupler curves so difficult to be traced directly in the workspace. The zoomed areas in Fig. 9 show this effect by showing how two overlapping branches next to a ramphoid cusp and a near-quadruple point are generated. A similar situation of this phenomenon arises for the path followed by P_9 from the initial configuration $s_{2,4} = 74$, $s_{1,6} = 122$, and $\eta = 14$. In this case a cusp and a tacnode can be identified (Fig. 10).

A different connected component of the coupler curve is obtained when starting from $s_{2,4} = 74$, $s_{1,6} = 98.92$, and $\eta = 0$ (Fig. 11). Observe how in this case a smooth simple curve in the distance space maps onto the Cartesian space as a curve with several singular points in a reduced area which would be almost impossible to be correctly traced using a standard predictor-corrector procedure.

As shown in the above example, the main advantage of the proposed two-step method for tracing the coupler curves of pin-jointed linkages is that the curves in the distance space can be decomposed into easy-to-trace non-self-intersecting branches. Actually, in the presented example all singularities arise when mapping these curves onto the Cartesian space.

4 CONCLUSION

The current approaches for tracing the coupler curves of plane mechanisms provide a rapid algebraization of the problem thus becoming blind to the underlying geometry. A new approach, based on a coordinate-free formulation, that looks first for the reachable configuration in a space of squared distances and then maps the result onto the workspace of the simulated mechanism has been presented. The used coordinate-free formulation involves products, additions, and square roots. The presence of square roots permits a more compact representation than the standard techniques based on polynomials. Square roots actually play a fundamental role in the presented approach because their sign represent the orientation of triangles formed by sets of three joints of the mechanism thus retaining important geometric information. The coupler curves are thus decomposed into segments where the signs of the oriented areas of the involved triangles remain invariant. This decomposition, besides providing a new insight in the analysis of coupler curves, avoids most of the possible drifts that could arise when using a standard predictor-corrector method directly in the workspace of the mechanism. These advantages have been exemplified by tracing the coupler curves of a double butterfly linkage.

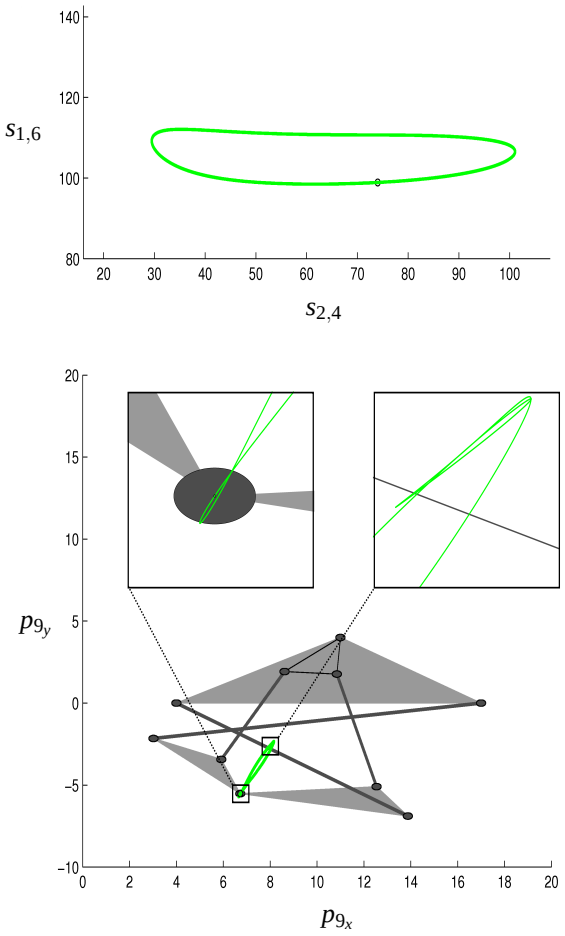

FIGURE 11. Top: Values reached by $s_{2,4}$ and $s_{1,6}$ in the analyzed double butterfly linkage when starting from the configuration $s_{2,4} = 74$, $s_{1,6} = 98.92$, and $\eta = 0$. Bottom: The corresponding Cartesian path traced by P_9.

ACKNOWLEDGMENT

We gratefully acknowledge the financial support of the Autonomous Government of Catalonia through the VALTEC program, cofinanced with FEDER funds, and the Colombian Ministry of Communications and Colfuturo through the ICT National Plan of Colombia.

REFERENCES

[1] Freudenstein, F., 1962. "On the variety of motions generated by mechanisms". *Journal of Engineering for Industry,* ***39***(February), pp. 156 – 160.

[2] Dhingra, A., Almadi, A., and Kohli, D., 2000. "Closed-form displacement analysis of 8, 9 and 10-link mechanisms: Part I: 8-link 1-DOF mechanisms". *Mechanism and Machine Theory,* ***35***(6), pp. 821 – 850.

[3] Gomes, A., Voiculescu, I., Jorge, J., Wyvill, B., and Galbraith, C., 2009. *Implicit Curves and Surfaces: Mathematics, Data Structures and Algorithms*, 1st ed. Springer Publishing Company, Incorporated.

[4] Walker, R., 1978. *Algebraic Curves*. Springer-Verlag.

[5] Allgower, E., and Georg, K., 2003. *Introduction to Numerical Continuation Methods*. SIAM.

[6] Sommese, A., and Wampler, C., 2005. *The Numerical Solution of Systems of Polynomials Arising in Engineering and Science*. World Scientific.

[7] Merlet, J., 2000. "Alias: An interval analysis based library for solving and analyzing system of equations". In Proceedings of the SEA.

[8] Porta, J., Ros, L., Creemers, T., and Thomas, F., 2007. "Box approximations of planar linkage configuration spaces". *Journal of Mechanical Design,* ***129***(4), pp. 397–405.

[9] Hernandez, A., and Petuya, V., 2004. "Position analysis of planar mechanisms with R-pairs using a geometrical-iterative method". *Mechanism and Machine Theory,* ***39***(2), pp. 133 – 152.

[10] Lambert, J., 1991. *Numerical Methods for Ordinary Differential Systems: The Initial Value Problem*. John Wiley and Sons.

[11] Morgado, J., and Gomes, A., 2004. "A derivative-free tracking algorithm for implicit curves with singularities". In International Conference on Computational Science, pp. 221–228.

[12] Hunt, K., 1978. *Kinematic Geometry of Mechanisms*. Clarendon Press, Oxford.

[13] Pennock, G., and Hasan, A., 2002. "A polynomial equation for a coupler curve of the double butterfly linkage". *Journal of Mechanical Design,* ***124***(1), pp. 39–46.

[14] Blumenthal, L., 1953. *Theory and Applications of Distance Geometry*. Oxford University Press.

[15] Rojas, N., and Thomas, F., 2011. "Distance-based position analysis of the three seven-link Assur kinematic chains". *Mechanism and Machine Theory,* ***46***(2), pp. 112 – 126.

[16] Rojas, N., and Thomas, F. "A review on the position analysis of Baranov trusses and closed-form solutions using the bilateration method". *In preparation*.

[17] McCarthy, J., and Soh, G., 2011. *Geometric Design of Linkages*. Springer.

[18] Pennock, G., and Raje, N., 2004. "Curvature theory for the double flier eight-bar linkage". *Mechanism and Machine Theory,* ***39***(7), pp. 665 – 679.